physica status solidi

pss

www.pss-journals.com

reprint

WILEY-VCH

Phys. Status Solidi B **248**, No. 11, 2631–2634 (2011) / **DOI** 10.1002/pssb.201100242

physica status solidi b
www.pss-b.com
basic solid state physics

Theory and model analysis of spin relaxation time in graphene — Could it be used for spintronics?

Ferenc Simon[*,1,3], **Ferenc Murányi**[2], **and Balázs Dóra**[1]

[1] Budapest University of Technology and Economics, Institute of Physics and Condensed Matter Research Group of the Hungarian Academy of Sciences, 1521 Budapest, Hungary
[2] Physik-Institut der Universität Zürich, Winterthurerstrasse 190, 8057 Zürich, Switzerland
[3] Fakultät für Physik, Universität Wien, Strudlhofgasse 4, 1090 Wien, Austria

Received 20 June 2011, revised 24 August 2011, accepted 29 August 2011
Published online 26 September 2011

Keywords carbon nanotubes, electron spin resonance, graphene, spin-decoherence, spin-lifetime, spintronics

* Corresponding author: e-mail ferenc.simon@univie.ac.at, Phone: +36-1-4633816, Fax: +36-1-4634180

Graphene appears to be an excellent candidate for spintronics due to the low spin–orbit coupling in carbon, the two-dimensional nature of the graphene sheet, and the high electron mobility. However, recent experiments by Tombros et al. [Nature **448**, 571 (2007).] found a prohibitively short spin-decoherence time in graphene. We present a comprehensive theory of spin decoherence in graphene including intrinsic, Bychkov–Rashba, and ripple related spin–orbit coupling. We find that the available experimental data can be explained by an intrinsic spin–orbit coupling which is orders of magnitude larger than predicted in first principles calculations. We show that comparably large values are present for structurally and electronically similar systems, MgB_2 and Li intercalated graphite. The spin-relaxation in graphene is neither due to the Elliott–Yafet nor due to the Dyakonov–Perel mechanism but a smooth crossover between the two regimes occurs near the Dirac point as a function of the chemical potential.

1 Introduction The discovery of graphene [1] stimulates interest due the fundamentally and technologically important properties. A potential application is spintronics [2], i.e., when the spin degree of freedom of electrons is utilized as information carrier. The principal parameter governing spintronic utility is the spin-relaxation time (also called as spin-lattice relaxation time), τ_s, which characterizes how a non-thermal equilibrium spin state decays. For applications, τ_s longer than 0.1–1 μs is required. An often cited concept is that "pure materials made of light elements" can reach this limit. The huge mobility of charge carriers in graphene (approaching $10^6\,cm^2/Vs$ [3]), the lightness of carbon, and the low-dimensionality of graphene are the reasons for the high expectations for its spintronic applications. This is supported by the long spin relaxation time in light metals such as, e.g., Li [4] or in low-dimensional conductors [5].

It therefore came as a surprise that τ_s as short as 60–150 ps are observed in spin transport experiments on graphene [6, 7], which renders it unusable for spintronics. The understanding of this result is therefore of great importance. More recent similar spin transport experiments indicate that the sample preparation has an important effect on the measured τ_s [8]. Here, we intend to make no judgment on the validity of the spin transport experiments and we focus on the results of Ref. [6] and we consider it as being intrinsic to graphene. Alternative scenarios suggested the effect of the substrate [9] or impurities [10] to explain the unexpectedly small τ_s found in Ref. [6].

Theories of spin relaxation are split into two classes: materials with inversion symmetry (e.g., Na or Si) and to materials where the inversion symmetry is broken either in the bulk (e.g., III–V semiconductors such as GaAs) or in two-dimensional heterostructures. The Elliott–Yafet (EY) theory [11, 12] explains the former case, where only intrinsic (i.e., atomic) spin–orbit coupling (SOC) is present, L_i, and predicts that spin ($\Gamma_s = \hbar/\tau_s$) and momentum relaxation rates ($\Gamma = \hbar/\tau$, τ is the momentum relaxation time) are proportional: $\Gamma_s = \alpha_i (L_i^2/\Delta^2)\Gamma$. Here $\alpha_i = 1 \ldots 10$ is band structure dependent [4], Δ is the energy separation of a neighboring and the conduction band.

The relaxation for broken inversion symmetry is explained by the Dyakonov–Perel (DyP) theory. It applies either when the symmetry breaking is in the bulk (the Dresselhaus SOC [13], L_D) or when it happens for a heterolayer structure (the Bychkov–Rashba SOC [14, 15], L_{BR}). The DyP theory shows that the spin and momentum relaxation rates are inversely proportional: $\Gamma_s = \alpha_{D/BR} L^2_{D/BR}/\Gamma$, where $\alpha_{D/BR} \approx 1$.

A link between the EY and the DyP was found recently [16]: for metals with inversion symmetry but rapid momentum scattering, the generalization of the EY theory leads to $\Gamma_s = \alpha_i (L_i^2/(\Delta^2 + \Gamma^2))\Gamma$, which gives a DyP like spin relaxation when $\Gamma > \Delta$.

Three types of SOC are present in graphene: intrinsic, BR (due to a perpendicular electric field), and the ripple related (which is due to the inevitable ripples in graphene). However, the role and magnitude of these SOC parameters is a debated issue. Estimates for the intrinsic SOC ranges two orders of magnitude; 0.9–200 μeV [17–19], whereas value of the BR SOC appears to be settled to 10–36 μeV per V/nm (Refs. [18] and [17], respectively). The effect of the substrate for the spin relaxation is also unsettled [9]. Given this debate, a description is required which enables comparison with the spin transport data.

Here, we present a theory of spin relaxation in graphene including intrinsic, BR, and ripple related SOC. We analyze the spin transport data from Refs. [6, 7, 20] and we find that the intrinsic SOC dominates the relaxation with a large, unexpected magnitude. We discuss two similar honeycomb systems; MgB_2 and LiC_6, and show that they exhibit similar intrinsic SOC. The result predicts a strong anisotropy of the spin relaxation time, which is, however, not fully supported by more recent experiments [7, 20].

2 Results and discussion Low energy excitations around the K point of the Brillouin zone are described by a two-dimensional Dirac equation:

$$H = v_F(\sigma_x p_x + \sigma_y p_y), \tag{1}$$

with the $v_F \approx 10^6$ m/s Fermi velocity [1]. The spin–orbit interaction in graphene is given by [17]:

$$H_{SO} = L_i \sigma_z S_z + \frac{L_{BR} + L_{ripple}(r)}{2}\left(\sigma_x S_y - \sigma_y S_x\right), \tag{2}$$

where L_i, L_{BR}, and L_{ripple} are the SOC's of the intrinsic, BR, and ripple terms, respectively. $L_{ripple}(\boldsymbol{r})$ is Gaussian correlated random variable, $\langle L_{ripple}(\boldsymbol{r}) L_{ripple}(\boldsymbol{r}')\rangle \sim \delta(\boldsymbol{r} - \boldsymbol{r}')$.

The spin relaxation rates induced by these SOC's are additive in lowest order provided

$$\max(L_i, L_{BR}, L_{ripple}) \ll \max(\Gamma, \mu), \tag{3}$$

which means

$$\Gamma_s = \Gamma_{s,i} + \Gamma_{s,BR} + \Gamma_{s,ripple}. \tag{4}$$

The contributions from the intrinsic ($\Gamma_{s,i}$), BR ($\Gamma_{s,BR}$), and ripple ($\Gamma_{s,ripple}$) relaxation rates are obtained using the Mori–Kawasaki formula similar to that used in Ref. [21] considering the conical band structure and the K, K' degeneracy:

$$\Gamma_{s,i} = \delta_{\nu,\parallel} \frac{L_i^2 \arctan(\mu/\Gamma)}{2\pi\mu\,\tilde{\mu}(\mu,\Gamma)}\Gamma, \tag{5}$$

$$\Gamma_{s,BR} = \frac{(2\delta_{\nu,\perp} + \delta_{\nu,\parallel})L_{BR}^2}{16\pi\tilde{\mu}(\mu,\Gamma)}\left[1 + \left(\frac{\mu}{\Gamma} + \frac{\Gamma}{\mu}\right)\arctan\left(\frac{\mu}{\Gamma}\right)\right], \tag{6}$$

$$\Gamma_{s,ripple} = \frac{(2\delta_{\nu,\perp} + \delta_{\nu,\parallel})\pi}{32} L_{ripple}^2 \rho(\mu,\Gamma), \tag{7}$$

$\nu = \parallel$, or $\perp$ is the spin polarization direction with respect to the graphene plane; e.g., $\nu = \parallel$ in the spin transport experiments [6]. Here, μ is the chemical potential and $\tilde{\mu}(\mu,\Gamma) = -\frac{\Gamma}{\pi}\ln\left(\frac{\mu^2+\Gamma^2}{D^2}\right) + |\mu|\left(1 - \frac{2}{\pi}\arctan\left(\frac{\Gamma}{|\mu|}\right)\right)$ is the pseudo chemical potential ($D \approx 3$ eV is the cutoff in the continuum theory) which appears in the expression of the density of states (DOS), $\rho(\mu,\Gamma)$, with finite μ and Γ:

$$\rho(\mu,\Gamma) = \frac{2A_c\tilde{\mu}(\mu,\Gamma)}{\pi\hbar^2 v_F^2}, \tag{8}$$

with $A_c = 5.24$ Å^2/(2 atoms) being the elementary cell and $\rho(\mu,\Gamma)$ is measured in units of states/eV atom.

The intrinsic contribution disappears when spins are polarized perpendicular to the plane and the BR and ripple terms have a 2:1 anisotropy for the $\perp$: $\parallel$ directions. For the intrinsic part, $\Gamma_{s,i} \approx (L_i^2/(2\mu)^2)\Gamma$ when $\mu \gg \Gamma$, which is an Elliott–Yafet like result with $\alpha_i = 1$ since the conduction band is separated from the nearest lying valence band (at the Fermi-wavenumber) by $\Delta = 2\mu$. In the vicinity of the Dirac point, DP (i.e., $\mu \approx 0$ and Γ finite) it returns a Dyakonov–Perel like result of $\Gamma_{s,i} = (L_i^2/[4\ln(D/\Gamma)])(1/\Gamma)$. This is in agreement with the generalized Elliott–Yafet theory which predicts a similar crossover when the momentum scattering rate overcomes other energy scales [16]. Interestingly, the intrinsic contribution can be well fitted with a Lorentzian: $\Gamma_{s,i} \approx \alpha'(L_i^2\Gamma'/(\mu^2 + \Gamma'^2))$, where $\alpha' \approx 0.2 \ldots 0.4$ and $\Gamma'/\Gamma \approx 1 \ldots 2$ for typical values of μ and Γ.

The BR term is only present if a perpendicular electric field, E, is applied, which induces a BR SOC of $L_{BR} = \kappa E$ with κ values between 10 [18] and 36 μeV/(V/nm) [17]. The electric field changes μ through: $\mu = \sqrt{n\pi\hbar^2 v_F^2}$ where $n = \beta E$ is the carrier density and $\beta = 0.22\ (\mathrm{V\,nm})^{-1}$ for SiO_2 gate insulator [22]. This yields the BR SOC as a function of μ: $L_{BR}(\mu) \approx \kappa\mu^2\, 3.4\ \mathrm{V/eV^2 nm}$.

The ripple relaxation contribution depends on Γ only if $\mu \ll \Gamma$, where it resembles an EY relaxation: $\Gamma_{s,ripple} \propto L_{ripple}^2 \Gamma \ln(D/\Gamma)$.

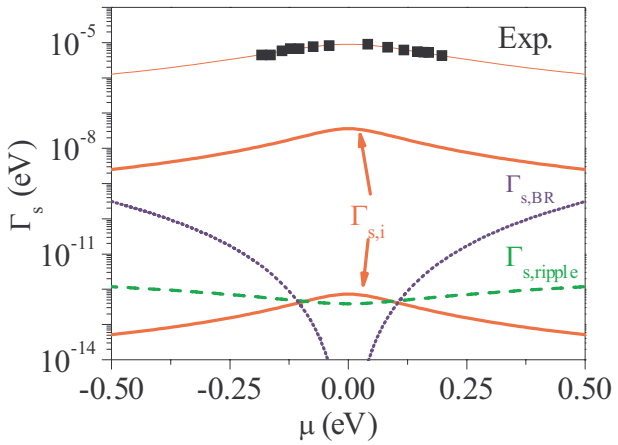

Figure 1 (online color at: www.pss-b.com) Experimental (symbols, from Ref. [20]) and calculated spin lattice relaxation rates, Γ_s, as a function of μ in graphene for in-plane spin polarization calculated with $\Gamma = 75$ meV after Ref. [20]. Upper (lower) solid curves are the maximal (minimal) estimates for the intrinsic contributions with SOC values from Refs. [17–19], respectively. Dotted curve is the BR contribution with the average of SOC values from Refs. [17, 18]. Dashed curve is the ripple contribution with L_{ripple} from Ref. [17]. The upmost thin solid line is a fit to the data as explained in the text.

In the following, we analyze the available spin transport data [6, 7, 20] in the framework of the above calculation. Values of $\tau_s = 60 \ldots 125$ ps were found around the charge neutrality point (depending on the sample), with a typical $\Gamma \approx 75$ meV [20]. Figure 1 shows the measured and calculated spin relaxation rate data for $v = \|$. $\Gamma = 75$ meV, that is independent of μ, was used for the calculated curves. First principles calculations of the intrinsic SOC scatter more than two orders of magnitude with values of 0.9 μeV [17, 23, 24], 24 μeV [18], and 200 μeV [19]. Values for the BR SOC, $L_{BR} = \kappa E$, vary between $\kappa = 10 \ldots 36$ μeV/(V/nm). This gives rise to the minimal and maximal estimates for both types of the contributions as shown in Fig. 1. The ripple SOC was estimated to be 17 μeV in Ref. [17].

Clearly, the first principles based relaxation rates fall short of explaining the experimental observation. Of the three contributions, only the intrinsic one has a μ dependence that mimics the experiment, whereas the other two shows the opposite. It may appear that a fit to the data is ill defined, given the relatively large number of free parameters (Γ and 3 L's). However, to our surprise, the fit consistently yields the same, *robust* set of parameters, irrespective of starting values or the method used (least squares fitting or combined with a simulated annealing), which are: $L_i = 3.7(1)$ meV, $L_{BR} = L_{ripple} = 0$, $\Gamma = 120(5)$ meV. This robustness originates from the qualitative difference between the μ dependence of the different contributions. The obtained values satisfy the criterion for the perturbative approach and the value of Γ determined herein is in agreement with that obtained in Ref. [20].

The intrinsic SOC opens a bandgap of L_i in the excitation spectrum [18, 19] therefore it is natural to ask: why is not this gap observed experimentally? Two interrelated answers are in order: first, best quality samples to date are ballistic only on the (sub)micron scale, giving a momentum scattering rate of the order of meV's (or bigger), which can mask the gap [25]. Second, charge inhomogeneities (the so-called puddles) prevent us from reaching the Dirac point, the average minimal charge density is estimated [26] as 10^9 cm^{-2}, which gives an average $\mu \sim 4$ meV, capable of overwhelming the obtained gap.

The present analysis allows for the design of graphene based spintronic devices. For spins polarized perpendicular to the graphene plane, the intrinsic contribution vanishes thus resulting in a substantially longer spin relaxation time. For spins polarized in the graphene plane, Fig. 2 shows that around the Dirac point purer samples (i.e., smaller Γ) decreases τ_s rather than increasing it, thus deteriorating performance. This, somewhat counterintuitive phenomenon, is the consequence of the Dyakonov–Perel like behavior of the intrinsic contribution around the DP.

The large value obtained for the intrinsic SOC is surprising as it is an order of magnitude larger than the largest theoretical estimate [19] and up to 3 orders of magnitude larger than other results [17, 23, 24]. However, given that the experimental μ dependence of Γ_s dictates the dominant role of the intrinsic coupling, L_i yields necessarily a large value. In the following, we consider two similar systems, MgB_2 and Li doped graphite and show that therein similar values of the intrinsic coupling are obtained.

In MgB_2, the boron atoms form a honeycomb lattice with four p-shell electrons, such as in graphene, which highlights the similarity of the two materials. Therein, an intrinsic SOC of $L_i(MgB_2) = 2.8$ meV of the π orbitals was found [21].

It was shown by Grüneis et al. [27] and confirmed [28] that alkali atom intercalated graphite is an excellent model

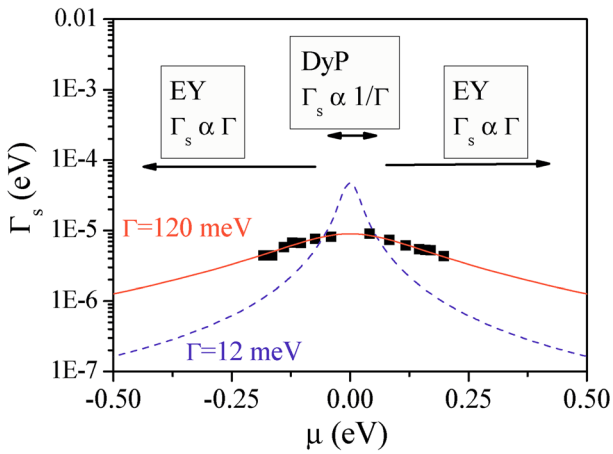

Figure 2 (online color at: www.pss-b.com) The same experimental data as in Fig. 1 shown along with the fit (solid curve). For comparison, Γ_s calculated with $\Gamma = 12$ meV (dashed curve) is shown. Arrows depict the crossover of the DyP and EY mechanisms as a function of μ.

system of biased graphene as the two-dimensional electron dispersion is retained due to the weak interlayer coupling. The Li intercalated stage I graphite compound LiC_6 [29] is particularly suitable to determine the intrinsic SOC as Li is the lightest alkali metal and its contribution to the spin relaxation is undetectable [4]. $L_i(LiC_6) = 1.1$ meV was obtained for the intrinsic SOC in LiC_6 [30]. The similar value of the intrinsic SOC in these three systems leads us to conclude that the intrinsic SOC is properly determined in graphene herein.

3 Summary In summary, a theory of spin relaxation in graphene is presented including intrinsic, Bychkov–Rashba, and ripple related spin–orbit coupling contributions. Analysis of the available spin transport data yields that the intrinsic contribution dominates. Interestingly, tuning the chemical potential makes the appearance of the relaxation change from the Dyakonov–Perel to the Elliott–Yafet spin relaxation mechanism. We finally note that a fruitful avenue to decide about the true magnitude of the spin-relaxation time could be its direct measurement by means of electron spin resonance spectroscopy such as reported in Ref. [31].

Acknowledgements This work supported by the Hungarian State Grants (OTKA) No. K72613, CNK80991, and K73361, by the ERC Grant No. ERC-259374-Sylo, and by the New Széchenyi Plan No. TÁMOP-4.2.1/B-09/1/KMR-2010-0002. BD acknowledges the Bolyai programme of the Hungarian Academy of Sciences. The Swiss NSF is acknowledged for support.

References

[1] K. S. Novoselov, A. K. Geim, S. V. Morozov, D. Jiang, Y. Zhang, S. V. Dubonos, I. V. Grigorieva, and A. A. Firsov, Science **306**, 666–669 (2004).
[2] I. Žutić, J. Fabian, and S. D. Sarma, Rev. Mod. Phys. **76**, 323–410 (2004).
[3] K. I. Bolotin, K. J. Sikes, Z. Jiang, M. Klima, G. Fudenberg, J. Hone, P. Kim, and H. L. Stormer, Solid State Commun. **146**, 351–355 (2008).
[4] F. Beuneu and P. Monod, Phys. Rev. B **18**, 2422 (1978).
[5] L. Forró, G. Sekretarczyk, M. Krupski, D. Schweitzer, and H. Keller, Phys. Rev. B **35**, 2501–2504 (1987).
[6] N. Tombros, C. Józsa, M. Popinciuc, H. T. Jonkman, and B. J. van Wees, Nature **448**, 571–574 (2007).
[7] N. Tombros, S. Tanabe, A. Veligura, C. Józsa, M. Popinciuc, H. T. Jonkman, and B. J. van Wees, Phys. Rev. Lett. **101**, 046601-1-4 (2008).
[8] W. Han, K. Pi, K. M. McCreary, Y. Li, J. J. I. Wong, A. G. Swartz, and R. K. Kawakami, Phys. Rev. Lett. **105**, 167202 (2010).
[9] M. Gmitra, S. Konschuh, C. Ertler, C. Ambrosch-Draxl, and J. Fabian, Phys. Rev. B **80**, 235431 (2009).
[10] A. H. Castro Neto and F. Guinea, Phys. Rev. Lett. **103**, 026804 (2009).
[11] R. J. Elliott, Phys. Rev. **96**, 266–279 (1954).
[12] Y. Yafet, Phys. Lett. A **98**, 287–290 (1983).
[13] G. Dresselhaus, Phys. Rev. **100**, 580–586 (1955).
[14] Y. A. Bychkov and E. I. Rashba, J. Phys. C **17**, 6039–6045 (1984).
[15] Y. A. Bychkov and E. I. Rashba, JETP Lett. **39**, 78–81 (1984).
[16] B. Dóra and F. Simon, Phys. Rev. Lett. **102**, 137001-1-4 (2009).
[17] D. Huertas-Hernando, F. Guinea, and A. Brataas, Phys. Rev. B **74**, 155426 (2006).
[18] C. Ertler, S. Konschuh, M. Gmitra, and J. Fabian, Phys. Rev. B **80**, 041405 (2009).
[19] C. L. Kane and E. J. Mele, Phys. Rev. Lett. **95**, 226801 (2005).
[20] C. Józsa, T. Maassen, M. Popinciuc, P. J. Zomer, A. Veligura, H. T. Jonkman, and B. J. van Wees, Phys. Rev. B **80**, 241403(R)-1-4 (2009).
[21] F. Simon, B. Dóra, F. Murányi, A. Jánossy, S. Garaj, L. Forró, S. Bud'ko, C. Petrovic, and P. C. Canfield, Phys. Rev. Lett. **101**, 177003-1-4 (2008).
[22] J. Fernández-Rossier, J. J. Palacios, and L. Brey, Phys. Rev. B **75**, 205441-1-8 (2007).
[23] H. Min, J. E. Hill, N. A. Sinitsyn, B. R. Sahu, L. Kleinman, and A. H. MacDonald, Phys. Rev. B **77**, 165310-1-5 (2006).
[24] Y. Yao, F. Ye, X. L. Qi, S. C. Zhang, and Z. Fang, Phys. Rev. B **75**, 041401 (2007).
[25] A. H. Castro Neto, F. Guinea, N. M. Peres, K. S. Novoselov, and A. K. Geim, Rev. Mod. Phys. **81**, 109 (2009).
[26] B. E. Feldman, J. Martin, and A. Yacoby, Nature Phys. **5**, 889–893 (2009).
[27] A. Grueneis, C. Attaccalite, A. Rubio, D. V. Vyalikh, S. L. Molodtsov, J. Fink, R. Follath, W. Eberhardt, B. Buechner, and T. Pichler, Phys. Rev. B **79**(20), 205106 (2009).
[28] Z. H. Pan, J. Camacho, M. Upton, A. Fedorov, A. Walters, C. Howard, M. Ellerby, and T. Valla, Phys. Rev. Lett. **106**, 187002 (2011).
[29] M. S. Dresselhaus and G. Dresselhaus, Adv. Phys. **51**, 1–186 (2002).
[30] A. H. Castro Neto and F. Guinea, Eur. Phys. Lett. **92**, 17002 (2010).
[31] L. Ćirić, A. Sienkiewicz, B. Náfrádi, M. Mionić, A. Magrez, and L. Forró, Phys. Status Solidi B **246**, 2558–22561 (2009).

